

The intrinsic electrical breakdown strength of insulators from first principles

Y. Sun,^{1,a)} S. A. Boggs,¹ and R. Ramprasad^{1,2}

¹*Institute of Materials Science, University of Connecticut, Storrs, Connecticut 06269, USA*

²*Chemical, Materials, and Biomolecular Engineering, University of Connecticut, Storrs, Connecticut 06269, USA*

(Received 22 August 2012; accepted 14 September 2012; published online 27 September 2012)

A first principles quantum-mechanical method for estimating intrinsic breakdown strength of insulating materials has been implemented based on an average electron model which assumes that the breakdown occurs when the average electron energy gain from the electric field exceeds the average energy loss to phonons. The approach is based on density functional perturbation theory and on the direct integration of electronic scattering probabilities over all possible final states, with no adjustable parameters. The computed intrinsic breakdown field for several prototypical materials compares favorably with available experimental data. This model also provides physical insight into the material properties that affect breakdown. © 2012 American Institute of Physics. [<http://dx.doi.org/10.1063/1.4755841>]

The dielectric breakdown of insulating materials has been a subject of experimental and theoretical investigations for many decades as a result of its technical importance.¹ Breakdown mechanisms are complex as they are dominated by “extrinsic” factors not inherent to the material such as imperfections (e.g., chemical impurities at the atomic level, and cavities at the microscopic and macroscopic scales) as well as statistical variations in morphology and microstructure. The subject of the present contribution is the “intrinsic” breakdown strength of an insulator, a quantity that can be viewed as an intrinsic material property which provides an upper bound to the dielectric breakdown field. Experimentally, intrinsic breakdown can be obtained only under ideal conditions, when all extraneous influences have been eliminated, at which point, the breakdown strength is determined solely by the physical properties of the material and temperature. Developing a predictive theory of intrinsic breakdown is the first step in the path to predicting extrinsic breakdown strength, as well as achieving an improved understanding of the fundamental factors that control dielectric breakdown.

Intrinsic breakdown can be explained in terms of electron-avalanche theory,² which depends on the presence and creation of charge carriers capable of migration through the dielectric. A central tenet of this theory is that the only relevant scattering mechanism for charge carriers is electron-phonon interactions. Electrons gain energy from an external electric field between successive collisions with phonons. At low electric fields, the electron energy distribution achieves steady state, as the energy gain from the external electric field is balanced by energy loss from collisions with phonons. At a sufficiently high electric field, the electron energy increases indefinitely until a threshold is reached at which a high-energy electron ionizes the lattice, leading to carrier multiplication. This process is referred to as impact ionization, and the ensuing avalanche of electrons can damage the material (e.g., through bond breakage). Within this framework, the breakdown criterion can be formulated following von Hippel^{1,3} as the lowest field at which the average

electron energy gain from the field is greater than the average energy loss to phonons for all electron energies less than that which produces impact ionization.

While quantum mechanical descriptions of intrinsic breakdown are well over 50 years old,^{1–5} until recently, the estimation of the relevant parameters, such as electron-phonon scattering rates, has relied on approximations or empirical deformation potentials.^{2,5,6} Here, we present a parameter-free scheme for estimating intrinsic breakdown strength by determining the electron energy gain and loss rates using density functional perturbation theory (DFPT). This scheme has been applied to a number of prototypical covalent and ionic materials, and the computed values of intrinsic breakdown are compared to the best available experimental data (Fig. 1). As can be seen from Fig. 1, the favorable agreement between calculations and experiments spans two orders of magnitude in the breakdown field. A second important outcome of this work is the correlation between the intrinsic breakdown strength and properties such as the bandgap and the phonon cut-off frequency. Such correlations provide a rational approach to screen for insulators with large intrinsic breakdown strength.

In the present work, the intrinsic breakdown field, F_{bd} , is defined according to the von Hippel low energy criterion.^{1,3} If we represent the rate of energy gain of an electron of energy E as $A(F, E)$ at a field F , and the rate of energy loss as $B(E)$, the above criterion can be written as

$$A(F, E) > B(E), \quad \text{for all } E \in \{\text{CBM}, \text{CBM} + E_g\}, \quad (1)$$

where CBM and E_g are the conduction band minimum and the bandgap of the material, respectively. The reason for choosing $\text{CBM} + E_g$ as the upper bound is that all electrons with greater energy will impact ionize the lattice leading to electron multiplication, i.e., $\text{CBM} + E_g$ is assumed to be the impact ionization threshold in the present treatment.

The rate of energy gain of an electron of energy E at field F can be evaluated as²

$$A(F, E) = \frac{e^2 \tau(E) F^2}{3m}, \quad (2)$$

^{a)}ying.sun@gradmail.ims.uconn.edu.

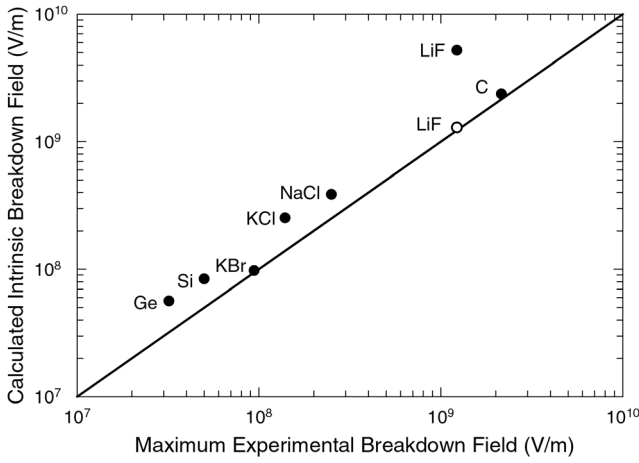


FIG. 1. Comparison of the maximum experimental breakdown field and the calculated intrinsic breakdown field for a range of covalently bonded and ionic materials. The data are tabulated in Table I. The filled circles indicate the computed intrinsic breakdown field when the impact ionization threshold is defined by the bandgap of the material (as per Eq. (1)). In the case of LiF, the enthalpy of formation (6.39 eV) is much lower than the bandgap (14.2 eV). It is thus expected that bond breakage will occur before impact ionization. The open circle in the case of LiF represents our result when the enthalpy of formation is used in Eq. (1) instead of the bandgap, as explained in the text.

where e and m are, respectively, the electronic charge and mass, and $\tau(E)$ is the electron relaxation time determined by scattering due to phonons. The isotropic (and purely energy dependent) form of the electron relaxation time (whose reciprocal is the scattering rate) is given by⁷

$$\frac{1}{\tau(E)} = \frac{1}{D(E)} \sum_{kj} \frac{1}{\tau(kj)} \delta(\varepsilon_{kj} - E), \quad (3)$$

where $D(E)$ is the electronic density of states, ε_{kj} is the energy of an electron above the CBM at wave vectors \mathbf{k} and band index j . The explicit \mathbf{k} - and j -dependent relaxation time, $\tau(kj)$ can be evaluated from Fermi's golden rule by direct integration of electronic scattering probabilities over all possible final states and is given by

$$\frac{1}{\tau(kj)} = \frac{2\pi}{\hbar} \sum_{q\lambda j'} |g_{k+qj',kj}^{q\lambda}|^2 \left(n_{q\lambda} + \frac{1}{2} \mp \frac{1}{2} \right) \times \delta(\varepsilon_{kj} - \varepsilon_{k+qj'} \pm \hbar\omega_{q\lambda}), \quad (4)$$

where \hbar is the Planck's constant and $\omega_{q\lambda}$ is the frequency of phonon at wave vector \mathbf{q} and band index λ . Physically, the above expression represents the scattering of an electron initially with energy ε_{kj} to a final state with energy $\varepsilon_{k+qj'}$ by a phonon with frequency $\omega_{q\lambda}$. The \pm sign indicates whether a phonon is absorbed (+) or emitted (-) during this scattering process. $n_{q\lambda}$ is the phonon occupation number which is given by the Bose-Einstein distribution. In the present study, we set $T = 300$ K for this distribution. The δ -function in the equation above ensures energy conservation during scattering,⁸ and $g_{k+qj',kj}^{q\lambda}$ is the electron-phonon coupling function⁷ given by

$$g_{k+qj',kj}^{q\lambda} = \sqrt{\frac{\hbar}{2M\omega_{q\lambda}}} |\langle \psi_{k+qj'} | \xi_{q\lambda} \cdot \nabla_{\mathbf{R}} V_{\mathbf{q}} | \psi_{kj} \rangle|^2, \quad (5)$$

where M is the atomic mass, $\xi_{q\lambda}$ are the phonon polarization vectors, $\nabla_{\mathbf{R}} V_{\mathbf{q}}$ is the gradient of the screened one electron potential with respect to atomic displacements from their equilibrium positions \mathbf{R} , and ψ_{kj} is the 1-electron wave function.

The net rate of energy loss $B(E)$ represents the energy exchange between an electron of energy E and the distribution of phonons (in terms of phonon emission or absorption) and can be calculated similarly to scattering rate as

$$B(E) = \frac{2\pi}{D(E)} \sum_{\pm} \sum_{kj} \sum_{q\lambda j'} \left\{ \pm \omega_{q\lambda} |g_{k+qj',kj}^{q\lambda}|^2 \left(n_{q\lambda} + \frac{1}{2} \mp \frac{1}{2} \right) \times \delta(\varepsilon_{kj} - \varepsilon_{k+qj'} \pm \hbar\omega_{q\lambda}) \delta(\varepsilon_{kj} - E) \right\}. \quad (6)$$

Combining Eqs. (1), (2), and (6) results in

$$F_{\text{bd}} = \text{Max} \left[\frac{\sqrt{3m}}{e} \sqrt{\frac{1}{\tau(E)} B(E)} \right], \quad E \in \{\text{CBM}, \text{CBM} + E_g\}. \quad (7)$$

The above approach provides the basis for estimating F_{bd} ,¹⁻³ provided $\tau(E)$ and $B(E)$ are available. In the present work, the relevant quantities are computed using first principles density functional theory (DFT) based calculations within the local density approximation (LDA) and norm conserving pseudopotentials as implemented in Quantum ESPRESSO.⁹ Phonon frequencies and the electron-phonon coupling function $g_{k+qj',kj}^{q\lambda}$ as defined in Eq. (5) were computed in the linear response regime using DFPT. Quantum ESPRESSO directly calculates $g_{k+qj',kj}^{q\lambda}$ which was then used to compute $\tau(E)$ and $B(E)$ as prescribed by Eqs. (3)–(6). For all the materials studied, the convergence of the calculations with respect to plane-wave cut-off energy, and the \mathbf{k} -point and \mathbf{q} -point meshes has been checked thoroughly. Accurate evaluation of $\tau(E)$ and $B(E)$ requires a very dense sampling of both the electronic (\mathbf{k}) and the phononic (\mathbf{q}) reciprocal space grids, significantly more dense than required in standard DFT computations involving the corresponding systems. The definitions of both $\tau(E)$ and $B(E)$ involve double delta functions, which, in practice, are replaced by sharp Gaussians. A Monkhorst-pack \mathbf{k} point mesh of $32 \times 32 \times 32$ and \mathbf{q} point mesh of $4 \times 4 \times 4$ with 0.01 Ry Gaussian broadening is used for all materials to obtain converged results. In polar materials, macroscopic electric fields are present in the long-wavelength limit and induce the so called LO-TO splitting as a result of the longitudinal optical phonons having a much greater frequency than transverse optical phonons. This effect can be accommodated in the computation by adding a non-analytic term to the dynamical matrix. Longitudinal optical phonon frequencies must be computed in order to provide the correct phonon frequencies for calculation of the polar electron phonon scattering rate.

Fig. 2 shows the electron-phonon scattering rate ($1/\tau(E)$) of Si computed here, along with the electronic density of states. The scattering rate follows closely the line shape of the density of states, and both quantities are generally in good agreement with prior work.^{7,10}

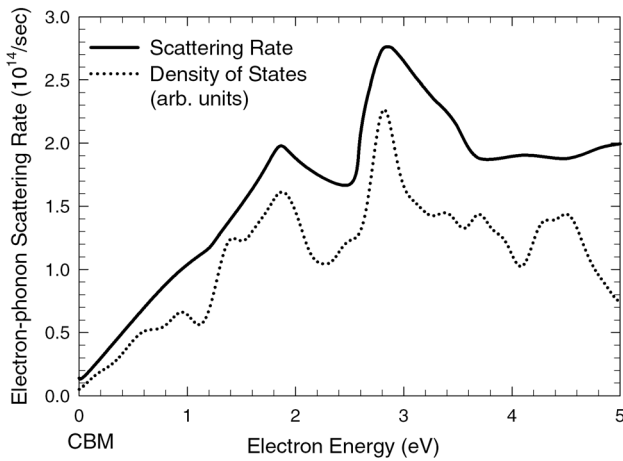


FIG. 2. The electron-phonon scattering rate ($1/\tau(E)$) and the density of states ($D(E)$) for Si at room temperature as a function of electron energy. The electron energy scale is referenced to the CBM.

Fig. 3 shows $A(F,E)$ and $B(E)$ (the former for various values of the electric field, F , as a function of the electron energy E . As prescribed by Eq. (1), the intrinsic breakdown field, F_{bd} , is the electric field at which the $A(F,E)$ curve is greater than the $B(E)$ curve over the entire energy range of interest, namely from the CBM to $\text{CBM} + E_g$. We use the experimental E_g value of 1.17 eV (for Si), as the LDA underestimates significantly the E_g of insulators. While advanced many-body methods can be used to compute E_g from first principles, we use available experimental E_g data for Si and other insulators considered here. The calculated F_{bd} of Si is 8.39×10^7 V/m compared with highest observed breakdown field of 5×10^7 V/m.¹¹

Using the same strategy, we have computed the intrinsic breakdown strength of other prototypical covalent systems including C and Ge (all in the diamond cubic structure), as well as ionic systems, such as LiF, NaCl, KCl, and KBr (all in the rocksalt structure). Our results, along with the maximum observed F_{bd} values, are plotted in Fig. 1 and tabulated in Table I. The large deviation of the calculated breakdown field for LiF with respect to experimental value can be explained by its large bandgap of 14.2 eV relative to its enthalpy of formation of 6.39 eV. Our model assumes that the electron in LiF gains energy from the electric field until it reaches a kinetic energy of 14.2 eV (the bandgap) at which

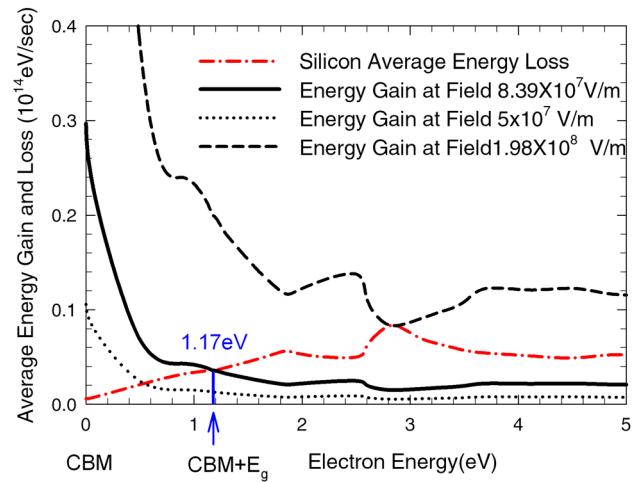


FIG. 3. The average energy loss ($B(E)$) and energy gain ($A(F,E)$) at electric fields of 5×10^7 V/m, 8.39×10^7 V/m, and 1.98×10^8 V/m for Si as a function of electron energy. The electron energy scale is referenced to the CBM. The intrinsic breakdown field of silicon is estimated as the electric field for which the energy gain curve (black solid line) is greater than energy loss curve (red dash-dot line) for all electron energies from the CBM to 1.17 eV above CBM, i.e., from the CBM to the CBM plus the bandgap (E_g) of Si.

point impact ionization leads to breakdown. In practice, an electron with such a high kinetic energy could break the Li-F bond (enthalpy of formation of LiF is 6.39 eV) before it reaches the impact ionization threshold energy. Accordingly, if the upper bound for electron energy in Eq. (1) is taken to be $\text{CBM} + 6.39$ eV (instead of $\text{CBM} + 14.2$ eV), the calculated breakdown field is 1.29×10^9 V/m which agrees well with the experimental breakdown field of 1.22×10^9 V/m as can be seen from Fig. 1.

A major difficulty in obtaining agreement between theory and experiment for the intrinsic breakdown field is determining whether the experimental data represent intrinsic breakdown. Breakdown fields from the literature for a given material vary substantially as a result of material defects and the experimental technique employed. The maximum breakdown field from reported data provides the best estimate of intrinsic breakdown strength. We note that the computed F_{bd} value represents the upper bound for intrinsic breakdown field. Electrical breakdown data for Si and Ge were obtained by measuring the current-voltage characteristics.^{11,14} The best available breakdown data for alkali halides

TABLE I. For all systems studied here, the calculated highest phonon frequency (in THz), and the breakdown field (in V/m) as per von Hippel's criterion are listed. The experimental bandgap (in eV), the highest observed breakdown field (in V/m), and the method adopted in such measurements are also listed.

	Phonon cutoff (THz)	Calculated intrinsic F_{bd} (V/m)	Expt. E_g (eV)	Expt. F_{bd} (V/m)
Ge	8.73	5.64×10^7	0.74 (Ref. 12)	^a 3.2×10^7 (Ref. 14)
Si	15.3	8.39×10^7	1.17 (Ref. 12)	^a 5×10^7 (Ref. 11)
C	37.9	2.37×10^9	5.48 (Ref. 12)	^b 2.15×10^9 (Ref. 15)
KBr	5.23	9.75×10^7	7.8 (Ref. 13)	^c 9.4×10^7 (Ref. 16)
KCl	6.88	2.53×10^8	8.5 (Ref. 13)	^c 1.39×10^8 (Ref. 16)
NaCl	8.13	3.86×10^8	8.6 (Ref. 13)	^c 2.5×10^8 (Ref. 2)
LiF	19.8	5.2×10^9	14.2 (Ref. 12)	^b 1.22×10^9 (Ref. 17)

^aElectrical breakdown.

^b1.06 μm laser breakdown.

^c10.6 μm laser breakdown.

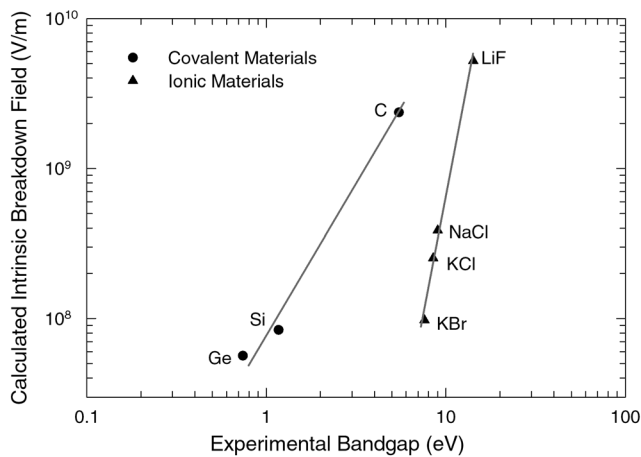


FIG. 4. Correlation between the calculated intrinsic breakdown field (F_{bd}) and the experimental bandgap (E_g).

are generated by optical breakdown measurements which eliminate the influence of many extraneous factors such as electrode interfaces. Most such optical measurements of breakdown field have been carried out at $10.6 \mu\text{m}$ or $1.06 \mu\text{m}$. The experimental data suggest that within experimental error, laser-induced breakdown and DC dielectric breakdown in insulators are identical processes.¹⁸ At $10.6 \mu\text{m}$, the frequency of the optical field is sufficiently low to be considered quasi-static in the context of phonon-induced electron energy relaxation. For high breakdown strength materials C and LiF, only $1.06 \mu\text{m}$ laser breakdown data are available in literature because of the greater power required to breakdown these materials. The characteristic electron relaxation time (which is the relaxation time used to determine F_{bd} in Eq. (7)) of C and LiF are calculated as $0.066 \times 10^{-14} \text{ s}$ and $0.014 \times 10^{-14} \text{ s}$, respectively, which is comparable or much smaller to the period of the electric field at $1.06 \mu\text{m}$ ($0.056 \times 10^{-14} \text{ s}$), which justifies the quasi-static limit for these two materials at $1.06 \mu\text{m}$.

In order to develop an intuition for the fundamental chemical and physical factors that control intrinsic breakdown, we examined the correlation of several easily computable attributes of the parent system with the computed F_{bd} values. Our results indicate that a clear correlation exists between F_{bd} and two fundamental properties, namely the bandgap and the highest phonon frequency (i.e., the phonon cutoff frequency). Attempts have been made in the past to correlate the bandgap with the maximum observed breakdown fields based on empirical data.¹⁹ This expectation is intuitive, as a material with a larger bandgap will display a higher threshold for impact ionization. Fig. 4 plots the computed F_{bd} and the experimental E_g (listed in Table I). As can be seen, a correlation between these two properties is evident, although the power law dependence appears to differ in exponent for the covalent and ionic systems. Nevertheless, the existence of such a correlation brings a measure of redemption to the qualitative notions proposed earlier.

Fig. 5 shows the dependence of F_{bd} on the phonon cutoff frequency (both of which are listed in Table I as well). Once again, a power law correlation is observed, although the ionic and covalent materials fall within differing groups. This dependence is also intuitively understandable. Materials

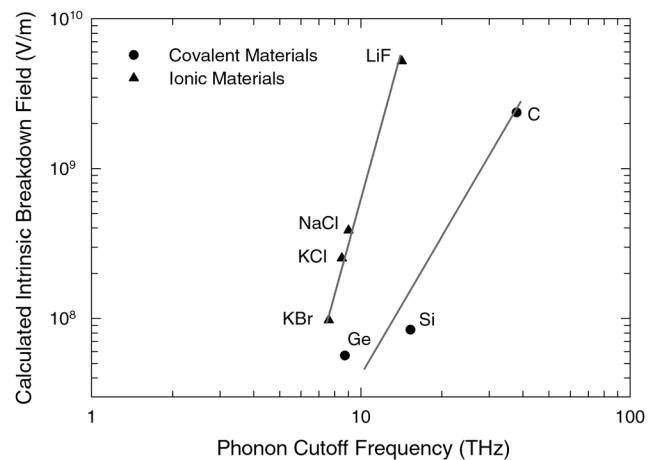


FIG. 5. Correlation between the calculated intrinsic breakdown field (F_{bd}) and the phonon cutoff frequency.

with greater phonon cutoff frequency tend to have greater average energy loss during each electron-phonon scattering event, leading to larger F_{bd} values. Thus, the intrinsic breakdown field is large for materials with large bandgap and/or large phonon cutoff frequencies. In the case of purely covalent systems, the bandgap is the more important factor, whereas in the case of highly ionic systems, the phonon cutoff frequency appears to be the more pertinent property.

Finally, we note that the computed electron relaxation times, $\tau(E)$, as defined in Eq. (3) (or the corresponding scattering rates, $1/\tau(E)$) has practical value. This quantity can be used in stochastic Monte Carlo based simulations of charge transport through the corresponding material (this has been attempted in the past, but such attempts have been based largely on empirical scattering rates^{20,21}). Such a Monte Carlo scheme can include effects due to defects (whose scattering rates need to be computed independently) and voids (within which no scattering occurs), thereby providing a first principles pathway to go beyond intrinsic breakdown.

In conclusion, a highly predictive parameter-free first principles method for estimating the intrinsic breakdown strength of insulators has been developed. This approach is based on the criterion that breakdown occurs when the average electron energy gain from the electric field exceeds average energy loss to phonon collisions. Density functional perturbation theory and the direct integration of electronic scattering probabilities (due to phonons) over all possible final states are used to arrive at an estimate of intrinsic breakdown for a range of prototypical covalent and ionic systems. The computed intrinsic breakdown fields compare favorably with available experimental data. This work also establishes correlations between the breakdown strength on the one hand and the bandgap and phonon cut-off frequencies on the other for the chosen material systems. These correlations, and the availability of first principles scattering rates provide a logical basis for the guidance of designing materials more resistant to damage from large electric fields.

Financial support of this work by a Multi-University Research Initiative (MURI) Grant from the Office of Naval Research (ONR) is gratefully acknowledged. The author would also like to acknowledge helpful discussions with Ghanshyam Pilania and Clive R Bealing.

- ¹R. Stratton, *Progress in Dielectrics 3*, edited by J. B. Birks and J. Hart (Wiley, New York, 1961), p. 235.
- ²M. Sparks, D. L. Mills, R. Warren, T. Holstein, A. A. Maradudin, L. J. Sham, E. Loh, Jr., and D. F. King, *Phys. Rev. B* **24**, 3519 (1981).
- ³A. Von Hippel, *J. Appl. Phys.* **8**, 815 (1937).
- ⁴H. Fröhlich, *Proc. R. Soc. London, Ser. A* **188**(1015), 521–532 (1947).
- ⁵H. Fröhlich, *Proc. R. Soc. London, Ser. A* **160**(901), 230–241 (1937).
- ⁶C. Jacoboni and L. Reggiani, *Rev. Mod. Phys.* **55**, 645 (1983).
- ⁷O. D. Restrepo, K. Varga, and S. T. Pantelides, *Appl. Phys. Lett.* **94**, 212103 (2009).
- ⁸J. Sjakste, N. Vast, and V. Tyuterev, *Phys. Rev. Lett.* **99**, 236045 (2007).
- ⁹P. Giannozzi, P. Giannozzi, S. Baroni, N. Bonini, M. Calandra, R. Car, C. Cavazzoni, D. Ceresoli, G. L. Chiarotti, M. Cococcioni, I. Dabo, A. D. Corso, S. de Gironcoli, S. Fabris, G. Fratesi, R. Gebauer, U. Gerstmann, C. Gougousis, A. Kokalj, M. Lazzeri, L. Martin-Samos, N. Marzari, F. Mauri, R. Mazzarello, S. Paolini, A. Pasquarello, L. Paulatto, C. Sbraccia, S. Scandolo, G. Sclauzero, A. P. Seitsonen, A. Smogunov, P. Umari, and R. M. Wentzcovitch, *J. Phys.: Condens. Matter* **21**, 395502 (2009).
- ¹⁰M. V. Fischetti, *IEEE Trans. Electron Devices* **38**, 634 (1991).
- ¹¹J. N. Park, K. Rose, and K. E. Mortenson, *J. Appl. Phys.* **38**, 5343 (1967).
- ¹²F. Tran and P. Blaha, *Phys. Rev. Lett.* **102**, 226401 (2009).
- ¹³R. T. Poole, J. G. Jenkin, J. Liesegang, and R. C. G. Leckey, *Phys. Rev. B* **11**, 5179 (1975).
- ¹⁴S. L. Miller, *Phys. Rev.* **99**, 1234 (1955).
- ¹⁵P. Liu, R. Yen, and N. Bloembergen, *IEEE J. Quantum Electron.* **QE-14**(8), 574 (1978).
- ¹⁶E. Yablonovitch, *Appl. Phys. Lett.* **19**, 495 (1971).
- ¹⁷W. L. Smith, J. H. Bechtel, and N. Bloembergen, *Phys. Rev. B* **12**, 706 (1975).
- ¹⁸L. H. Holway and D. W. Fradin, *J. Appl. Phys.* **46**, 279 (1975).
- ¹⁹L. M. Wang, *Proceedings of the 25th International Conference on Micro-electronics*, Belgrade, Serbia and Montenegro, 14–17 May (2006), p. 576.
- ²⁰H. K. Jung, K. Taniguchi, and C. Hamaguchi, *J. Appl. Phys.* **79**, 2473 (1996).
- ²¹F. Bertazzi, M. Moresco, and E. Bellotti, *J. Appl. Phys.* **106**, 063718 (2009).